Secretory pathway Ca-ATPase 2 (SPCA2) gene knockout results in mouse mammary gland changes and a secretory defect

Timothy Reinhardt (tim.reinhardt@usda.gov)
National Animal Disease Center, USDA/ARS
John Lippolis
National Animal Disease Center, USDA/ARS
Mitchell Palmer
National Animal Disease Center, USDA/ARS

Research Article

Keywords: mammary calcium transport, SPCA2 Knockout, secretory pathway Ca2-ATPase 2, mammary gland, lactation, milk production, mouse milk proteome, lactating mouse mammary proteome

Posted Date: August 26th, 2021

DOI: https://doi.org/10.21203/rs.3.rs-830264/v1

Abstract

Calcium influx into the basolateral mammary cell is thought to be due partly to an unconventional partnering of SPCA2 and the calcium channel protein ORAI1 in vitro. ORAI1's role in mammary secretory cell calcium influx, in support of milk calcium, has been confirmed in ORAI1 knockout (KO) mice. We examine the role of SPCA2 on mammary cell calcium influx in support of milk calcium concentration in SPCA2 KO mice. The SPCA2 KO resulted in a significant 40% reduction in milk calcium and a 57% reduction in milk manganese concentrations. The loss of SPCA2 was associated with a significant 55% increase in SPCA1, which may be compensatory. The expression of other calcium transporters/channels such as PMCA2/NHERF1, ORAI1, NCX1, and TMEM165 were not affected by the loss of SPCA2. Histologically SPCA2 KO mammary glands showed increased adiposity and altered structure. Milk production was significantly down in SPCA2 KO mice, but milk fat, protein, and lactose were unaffected. The significant decline in milk calcium in SPCA2 KO mice indirectly supports the SPCA2 role as an ORAI1 partner in calcium influx into mammary tissue. Further, studies will be required to clarify this relationship between SPCA2, ORAI1, and STIM1 on mammary calcium influx *in vivo*.

Introduction

The lactating mammary gland transports enormous amounts of Ca^{2+} from the blood to the milk via the mammary secretory cells[1]. Lactating mammary calcium homeostasis is challenging because mammary glands store 12–30 mmol Ca^{2+}/g tissue compared with less than 1 mmol/g in non-mammary tissues [2,3]. Calcium pumps [4–6], transporters [7,8] and ion channels[6,9,10] coordinate these complex transcellular Ca^{2+} fluxes during lactation to move large amounts of calcium from the blood through the secretory cell and into the milk while maintaining cellular calcium homeostasis in the face of this cell toxic ion [1,11]. The functional module controlling mass calcium fluxes in the mammary gland is termed Calcium movement by the calcium trans- porter (CALTRANS)[12,13] and includes calcium pumps, channels, transporters, sensors, buffers and associated functional partners to these proteins. Thus, the loss of these calcium regulators may lead to loss of cell calcium homeostasis and a concomitated loss of secretory cell function[4,8,9].

The secretory pathway Ca2+/Mn2+-ATPase 2 (SPCA2) protein was described in 2005 as Golgi localized but with a more restricted tissue expression than secretory pathway Ca2+/Mn2+-ATPase 1 (SPCA1)[14,15]. One of the tissues expressing large amounts of SPCA2 was the mammary gland but of unknown lactation status[15]. In subsequent studies, SPCA2 expression increased massively as milk production increased and is significantly downregulated as lactation ceases[6,16]. *In vitro* experiments with a mammosphere model of lactation demonstrated that SPCA2 and Oria1 mediate the basolateral calcium influx into mammary secretory cells to support the large calcium requirements of lactation via a store-independent entry (SICE) mechanism [6]. In other work using Orai1 knockout mice, it was concluded that Orai1 and the store-operated entry (SOCE) mechanism of calcium influx to cells are responsible for up to 50% of the calcium transported into secretory cells and that then ends up in the milk[9].

In the current study, loss of SPCA2 resulted in a 40% reduction of milk calcium and an 32% reduction in milk production. While these are significant lactation defects, we observed few other protein changes to account for the defects. An in-depth proteomic examination wild type milk and mammary tissue compared to milk and mammary tissue from SPCA2 knockouts provided little enlightenment to explain these lactation defects.

Results

Western blots were performed on day 13 lactating mammary tissue collected from mice of all three genotypes. SPCA2 expression in the 3 genotypes is shown in Fig. 1A&B. Heterozygote (HET) SPCA2 expression was down 52% ($P \leq 0.001$) compared to Wild Type mice (WT). SPCA2 expression was undetectable in lactating mammary tissue from knockout mice (KO) ($P \leq 0.001$). In contrast, SPCA1 relative expression increased 55% in KO mice compared to WT. The other Golgi Ca2+/Mn2 + transporter, TMEM165, essential in lactating mammary tissue, was unchanged by the SPCA2 KO (Fig. 1A, C&D).

Plasma membrane Ca2+-ATPase 2 (PMCA2) expression was unaltered by the loss of one or both SPCA2 alleles (Fig. 2A&B). Next, we examined the expression of NHERF1, which is known to partner with PMCA2 (Fig. 2A&C). NHERF1 expression was also unaltered in mammary tissue by losing one or both SPCA2 alleles, as was the sodium-calcium exchanger NCX1 (Fig. 2A&2D).

Figures 3A, B and C show that mammary ORAI1 was not affected by the loss of SPCA2, but ORAI1's protein partner STIM1 was significantly upregulated 39% ($P \leq 0.05$). Finally, E-Cadherin was unaffected by the loss of SPCA2 Fig. 3D).

General milk components such as milk fat, protein and lactose were unaffected by loss of mammary SPCA2 (Fig. 4A, B &C). However, milk production was significantly decreased in SPCA2 KO mice as indirectly measured by pup weight (Fig. 4D). Measurement of mammary tissue microsomes isolated from the 3 genotypes showed that SPCA2 KO mice tissue yielded significantly less microsome mass per gram tissue compared to WT and HET mice (Fig. 4E). This might be explained by a significant increase in measured adipose tissue in Mammary glands from SPCA2 KO mice Fig. 4F), which is visualized in Fig. 5.

Histological sections (4X) of mammary glands from HET mice were like those of wild-type mice (Fig. 5A), albeit there was a mild increase in the interstitial stroma and significant increase in adipose tissue (Figs. 4E and 5B) which is more evident in KO mice (Fig. 5C). Much of the gland contained active secretory alveoli variably filled with milk like those seen in wild-type mice (Fig. 5D). Outside of alveolar or ductal structures, among the stroma and adipose tissue in the KO mice, there was amphiphilic flocculent to highly vacuolated proteinaceous material consistent with milk (Fig. 5F). Also, within this interstitial stroma were low to moderate numbers of highly vacuolated cells and apoptotic cells. TUNNEL testing did not reveal any increase in apoptosis due to loss of SPCA2 (data not shown). A small number of alveoli were characterized by an incomplete epithelial lining void of epithelial cells, basement membrane, or surrounding myoepithelial cells resulting in a direct connection between alveolar lumens and interstitial spaces (Fig. 5F).

The effect of SPCA2 KO on milk cations is shown in Fig. 6. Milk calcium and manganese are significantly down 40 and 57% respectively in SPCA2 KO mice compared to WT mice (Fig. 6A&B). Milk zinc and iron are significantly down 22 and 24% respectively in SPCA2 KO mice (Fig. 6C&D). While milk copper was unaffected by genotype (Fig. 6E).

Due to the loss of mammary SPCA2, mouse tissue and milk whey proteomes were done to discover what other proteins might have altered expression due to the loss of SPCA2. Lactating mammary tissue proteomes comparing wild type vs. SPCA2 knockout mice can be found in Supplementary Table 1 under the imputed data tab. Of 3733 high confidence protein identifications, only 8 proteins were significantly differentially regulated between wild type and SPCA2 knockouts. Milk whey proteomes comparing wild type vs. SPCA2 knockout mice can be found in Supplementary Table 2 under the imputed data tab. Of 408 high confidence protein identifications, only 25 proteins were significantly differentially regulated between wild type and SPCA2 knockouts. Mammary crude membrane proteomes comparing wild type vs. SPCA2 knockout mice can be found in Supplementary Table 3 under the imputed data tab. Out of 1523 high confidence protein identifications, 39 proteins were significantly differentially regulated between wild type and SPCA2 knockouts. Few of the significantly differentially regulated proteins in all three proteomic sample sets stood out as having contributed to the SPCA2 knockout phenotype. The exception may be the significant downregulation of the tight junction protein ZO-1 from the cruse mammary membranes (Supplementary Table 3 under the imputed data tab). Only Osteopontin (gene name Spp1) and Immunoglobulin heavy constant alpha (gene name Igha) were common to the significantly differentially regulated proteins in mammary tissue and milk whey. Spp1 was significantly upregulated in mammary tissue and milk whey (Supplementary Tables 1 & 2), while Igha was significantly downregulated in SPCA2 knockout mammary tissue and milk whey (Supplementary Tables 1 & 2).

Discussion

SPCA1 and SPCA2 are both Golgi secretory pathway Ca2+/Mn2+-ATPases. However, SPCA2 has a more restricted tissue expression than the housekeeping form SPCA1[15]. Both SPCA1 & 2 are highly expressed in mammary tissue and the expression of both increases massively with milk production[6,16,17]. Functionally we know little about SPCA1 in lactation in part because SPCA1 knockout mice are not viable[18] and SPCA1 heterozygotes did not have a significant change in milk or mammary phenotype Reinhardt et al. unpublished). However, SPCA2 was found to increase the influx of calcium into breast tumor cells by SICE[10] and subsequent in vitro experiments with a cell model of lactation demonstrated that SPCA2 and Oria1 together mediate the basolateral calcium influx into mammary secretory cells to support the large calcium requirements of lactation via SICE[6]. In contrast, using Orai1 knockout mice, it was determined that Orai1 and the store-operated mechanism (SOCE) of calcium influx to secretory cells is responsible for up to 50% of the calcium transported into milk[9]. The current availability of a SPCA2 knockout mouse model has allowed us to examine the role of SPCA2 in lactation.

So, the general working hypothesis was that loss of SPCA2 (Fig. 1B) would at a minimum lead to reduced calcium in milk[8] due to reduced calcium entry into the secretory cells thus, providing less available calcium for secretion with milk. The loss of SPCA2 to partner with Orai1 resulted in SICE loss and a 40 % reduction in milk calcium (Fig. 6A). Therefore, SOCE is responsible for 50% of the calcium transported into milk[9] and SICE is responsible for 40%. That accounts for most of the calcium influx into the secretory cells via these two pathways. However, these in vivo gene deletion lactation models are not unambiguous enough to allow these conclusions. The Orai1 gene deletion paper did not consider the possibility of Orai1 partnering with SPCA2 to support SICE[6,9,12]. Only SOCE was considered as a mechanism for calcium influx into secretory cells and they noted that neither Orai2, Orai3, nor Stim1or Stim2 showed compensatory upregulation due to loss of Orai1[9]. Similarly, there was no or little compensatory upregulation most components of CALTRANS due to loss of SPCA2 with the notable exception of SPCA1 (Figs. 1, 2 and 3)

In non-gene deletion mouse lactation experiments, it has been shown that Orai1 expression rises as milk production increases, whereas Stim1 expression declines precipitously[19]. This might suggest that a classical partnering of Orai1 and Stim1 to support mM SOCE in lactation is not viable. However, Stim2 is upregulated with lactation, thus providing a possible partner to support SOCE. In contrast, our data support the SICE pathway. At this point, we can only conclude without further information that both SICE and SOCE contribute to the massive influx of calcium required to support normal milk production. Other calcium ion channels that regulate this enormous calcium influx may be necessary to support normal milk calcium, but this information awaits further research.

The primary lactation defect associated with loss of SPCA2 was reduced milk production as estimated by pup weights (Fig. 4D). Reduced milk production seems to be a common lactation defect when some CALTRANS genes are knocked out[4,8,9]. Histologically, the loss of SPCA2 resulted in mammary tissue adipocytes (Fig. 5E), a significant increase in % adipose tissue (Fig. 4F) and a measured reduction in tissue membrane content (Fig. 4E). All these likely contribute to the loss of milk production. We also observed that loss of SPCA2 lead to mammary alveoli with missing epithelial cells that allowed milk to leak into the interstitial spaces (Fig. 5E). This observation suggested loss of normal epithelial tissue structure and integrity, which is in part a function of E-Cadherin[20]. Recent work from Rao's lab[21] demonstrated that SPCA2 expression positively correlates with E-cadherin expression in breast cancer cells. Furthermore, in these breast cancer cells, loss of SPCA2 with the concomitant reduction in E-cadherin promoted an epithelial to mesenchymal cell transition, which might explain our apparent loss of epithelial tissue structure in mammary alveoli (Fig. 5E). However, in normal lactating mammary tissue, this relationship between SPCA2 and E-cadherin seems to be missing (Fig. 3D). The downregulation of the ZO-1 tight junction protein was the only observed protein change in SPCA2 knockouts that might contribute to the loss of epithelial tissue structure in mammary alveoli (Fig. 5E). Further work will need to be done to address this effect of SPCA2 loss.

Milk components such as protein, fat and lactose were unaffected in the SPCA2 knockout mice. This contrasted with the significant reduction of lactose and increase in milk protein in PMCA2 and TMEM165 KO[4,8]. The lactose reduction in PMCA KO mice was transient with no explanation. However, the reduction in lactose synthesis seen in TMEM165 was partly attributed to a marked decrease in manganese transport to milk in TMEM165 KO's that suggested reduced Golgi Manganese. Since manganese is a cofactor for lactose synthetase, it was concluded that, in part, the lack of manganese might have contributed to the reduced lactose seen in milk from TMEM165 KO[8]. Since a similar reduction in milk manganese was observed with the SPCA2 knockout (Fig. 6B) and milk lactose was not affected, we might assume that the TMEM165 effect on milk lactose was due to other factors such as TMEM165 proposed role in the regulation of Golgi pH[8].

In this SPCA2 KO experiment, there was some compensatory regulation of proteins that make up the CALTRANS module of calcium pumps, channels, transporters, sensors, binding proteins, and buffers[12,13]. Both SPCA1 and Stim 1 were moderately upregulated. Similar compensatory regulation was found following knocking out the PMCA2 gene, which resulted in compensatory upregulation of SPCA1 and SERCA2 in lactating mammary tissue[4]. A cell-based system overexpression of SPCA1 in COS-7 cells resulted in compensatory downregulation of pan-PMCA, calreticulin and CALNUC[22]. Despite compensatory upregulation of SPCA1 and Stim1 they were unable to compensate for the loss of SPCA2. SPCA1 as a Ca^{2+}/Mn^{2+} transporter clearly could not make up for the milk/cell Mn^{2+} deficit induced by loss of SPCA2.

To screen for members of CALTRANS more efficiently, we used a label-free proteomics approach to quantitate changes in the proteome between WT and KO mammary membranes, mammary whole cell lysates and milk whey. To our surprise, we found almost no compensatory regulated CALTRANS members with the loss of SPCA2 from lactating mammary glands (Supplementary Tables 1, 2 & 3 imputed tabs). Most of the differentially regulated proteins due to loss of SPCA2 could not, with our current knowledge, be directly related to the loss of SPCA2. The lone exception may be significant downregulation of potential CALTRANS member Inositol 1,4,5-trisphosphate receptor type 1 (Supplementary Table 3 imputed tab), which mediates the mediates calcium release from the endoplasmic reticulum. A reason for its downregulation would be speculation.

Osteopontin was found to be significantly upregulated following the loss of SPCA2 (Supplementary Tables 1 & 2 imputed tabs) in two of the proteome datasets. Osteopontin is an adhesive extracellular matrix protein whose loss results in abnormal mammary morphogenesis and defective lactation[23]. In contrast, in this study, Osteopontin is overexpressed following the loss of SPCA2. Adipose tissue is a known source of Osteopontin[24] and since the SPCA2 knockout tissue has significantly more adipose tissue (Fig. 4F&5E), this could be the reason we see more Osteopontin in SPCA2 KO mice. In breast cancer cells, Osteopontin increases both cell migration, cell invasiveness and metastasis[25,26]. Thus, the higher Osteopontin expression seen in SPCA2 KO could contribute to changes in mammary tissue described in Fig. 5E.

In conclusion, the significant decline in milk calcium following the loss of SPCA2 supports a role for SPCA2 in SICE. The loss of SPCA2 to partner with Orai1 resulted in a 40 % reduction in milk calcium. This significant decline in milk calcium following the loss of SPCA2 supports a role for SPCA2 in SICE in lactation with in vivo data. Additional studies will be required to clarify this relationship between SPCA2, ORAI1, and STIM1 on mammary calcium influx in vivo and the relative role of SICE and SOCE in mammary calcium influx to support calcium needs for lactation.

Methods

Guidelines

All procedures and methods used were carried out in accordance with relevant safety guidelines and recommendations.

Animal care and use

The National Animal Disease Center, USDA/ARS Institutional Animal Care and Use Committee (IACUP) approved all animal protocols and procedures following both the “Guide”[27] and ARRIVE[28] guidelines.

The SPCA2 knockout mice, C57BL/6N-Atp2c2 < em1(IMPC)Tcp>, were made as part of the KOMP2 phase 2 project at The Centre for Phenogenomics. The mice came from the Canadian Mouse Mutant Repository (http://phenogenomics.ca/index2.html?v=8). Pregnant and lactation mice plus pups were housed in hanging basket cages with soft cellulose bedding and enrichment. For genotyping, tail snips were collected from mice 17–25 days old. Tail snips were digested according to the instructions of the Sigma REDExtract-N-Amp tissue PCR kit and PCR was performed on the genomic DNA extract.

Genotyping

The mice were genotyped using the following primers in two independent reactions. The primers are Atp2-WT-F (5’-CCT AAG CTA AAT CAA GTC TCC TGC C -3’), ATP2-WT-R (5’-CTC CAG ACT TTA CAG CCC TAC TTT G -3’) [979 bp band present in wild-type and heterozygotes. Absent in homozygotes]. The second reaction, primers are Atp2-em1-F (5’ CCA CTAMGCT AAA TAA ACA GGC AGC – 3’), Atp2-em1-R (5’-TCT GTG GGA CTA ACT GTT CAG G- 3’) [909 and 1719 bp bands; only the larger band may be present in wild-type but may not be there in all wild-type mice; both bands may be present in heterozygotes, and only the smaller band is present in homozygotes].

Mouse milking

Milk was collected on day 12 of lactation as follows. Baby mice were removed from the mother for 3–4 hrs. before milk collection. Lactating mice were then anesthetized with an IP injection of Ketamine (100 mg/kg of BW) and Xylazine (10 mg/kg of BW). After they were anesthetized, the mice were given 1.0 IU of Oxytocin IP and 5 mins were allowed to pass before the start of milking. Milk was collected using a device made of small tubing connected to a 1.5 ml tube and a low vacuum that was pulsed. On day 13 of

lactation, the mice were anesthetized with a 50:50 mix of CO_2:O_2 followed by decapitation. Tissue was collected and stored at -80 C.

Inductively coupled plasma mass spectrometry measurements of milk calcium, manganese, zinc, iron and copper were performed in the Oregon Health & Science University Elemental Analysis Core facility with partial support from NIH (S10RR025512). Milk protein was determined using the BioRad Protein Assay Kit using a BSA standard. Milk lactose concentration was determined using a Lactose Assay Kit Cat # MAK017 (Sigma-Aldrich, St Louis MO). Milk fat concentration was estimated by cream-o-crit assay [29].

Mammary tissue whole cell lysates and microsomal membrane preparation.

Mammary tissue microsomes were prepared as previously described. Briefly, tissue was homogenized in 10 volumes of Buffer A, which contained: Trisma base (10 mM), MgCl2 (2 mM), EDTA (1 mM), and DL-dithiothreitol (2 mM) at pH 7.5.

The homogenate was mixed with an equal volume of Buffer B (Buffer A plus 0.5M Sucrose and 0.3 M KCl in place of the 2mM MgCl2) and centrifuged at 5,000 x g for 15 min. at 4C. The supernatant was collected, adjusted to 0.7 M KCl by adding solid KCl, and centrifuged at 200,000 x g for 40 min. The supernatant was discarded, and the pellets were resuspended in Buffer C (Buffer A plus 0.25M sucrose and 0.15 M KCl in place of 2 mM MgCl2). Membrane preparations were stored at − 70°C until assayed. Proteins were determined using the BioRad Protein Assay Kit using a BSA standard.

Mammary whole tissue lysates were prepared by homogenizing mammary tissue in 5 volumes of buffer A at 4C. This homogenate was mixed with 5 volumes of buffer B by homogenizing for 10 sec. The homogenates were then centrifuged at 1500 x g for 15 min at 4C. The supernatant was frozen at -80C. Proteins were determined using the BioRad Protein Assay Kit using a BSA standard.

Gel electrophoresis and Western blotting.

The methods were as described previously. Briefly, proteins for analysis were incubated for 10 min at 70C in a modified Laemmli buffer containing 150 mg/ml urea (8). Samples were then electrophoresed for 50 minutes at 200 volts in a 4–12% Novex NuPAGE® Bis-Tris Gel using MOPS SDS running buffer (Life Technologies, Grand Island, NY). Proteins were transferred to nitrocellulose membranes using the iBlot Dry Blotting System (Life Technologies, Grand Island, NY) at 23 volts for 6 minutes. Blots were developed using Pierce's Supersignal (Pierce Products, Rockford IL) using the protocol provided by the manufacturer. Blot images were collected using a LI-COR ODYSSEY Fc image analysis system (LI-COR, Lincoln NE). Blot quantitative analysis used the LI-COR Image Studio Software. Blots were probed with Abcam antibodies to Tubulin, Cat # ab4047, E-Cadherin, Cat # ab76055, NCX1, Cat # ab240203 and NHERF-1, Cat# ab88238, (https://www.abcam.com); Sigma antibody to TMEM165, Cat # HPA038299 (https://www.sigmaaldrich.com); Cell Signaling antibody to STIM1 (https://www.cellsignal.com); ThermoFisher antibody to Osteopontin, Cat # PA%-34579 (https://www.thermofisher.com/); Alomone

Labs antibody to ORAI1, Cat # ACC-062 (https://www.alomone.com/). The PMCA2 and SPCA1 antibodies used were described previously (REF). The SPCA2 antibody used was made using KLH conjugated peptide VRCGPKSEDGEDIYF-C in rabbits.

Milk production.

Milk production for the 3 genotypes was estimated indirectly by weighing the pups. Milk whey's were prepared as previously described [30]

Histological sections, staining and adipose morphometry

Mammary tissue was fixed in Tellyesniczky's fixative (a 20:2:1 ratio of 70% ethanol, formalin, and glacial acetic acid) for 5 hours before being stored in 70% ethanol before paraffin embedding and creation of 4 µm sections. For histological analysis and adipose tissue morphometry, slides of mammary gland stained with hematoxylin and eosin [31] were digitally scanned at 20X magnification using the Aperio ScanScope XT workstation (Aperio Technology, Inc., Vista, CA, USA). Digitized images were analyzed using image analysis software (HALO, Indica Labs, Inc., Corrales, NM). Each section of the mammary gland was selected as a region of interest and the whole area of the mammary gland was measured in μm^2., Adipose tissue within the mammary gland was then selected and the total area of adipose tissue was measured in μm^2. The percentage of each section of the mammary gland occupied by adipose tissue was then calculated. TUNNEL analysis was done a previously described[8].

Lys C and trypsin digests

We digested WT (n = 5) and KO (n = 5) whole cell lysates (100 µg each) and milk whey (100 ug each) with Trypsin/Lys-C Mix, Mass Spec Grade (Promega Corporation, Madison, WI) using the two-step in-solution digestion protocol outline in the manufacturer's instructions. Mammary crudes membranes from WT (n = 4) and KO (n = 4) were digest same as above for a proteome run on an older instrument. All the digests' samples were fractionated into eight subfractions using the Pierce High pH Reversed-Phase Peptide Fractionation Kit (Thermo Fisher Scientific, West Palm Beach, FL) following the manufacturer's instruction.

Peptide chromatography and mass spectroscopy

Peptide chromatography used a Thermo Dionex UltiMate 3000 RSLCnano system (Thermo Fisher Scientific, West Palm Beach, FL). The peptide digest subfractions for each genotype were chromatographed on an Acclaim PepMap 100 C18, 3 µm, 75 µm x 50 cm column in mobile phase A (95% H2O: 5% acetonitrile and 0.1% formic acid) and mobile phase B (5% H2O: 95% acetonitrile and 0.1% formic acid). The gradient was 1%B for 15 min, 1%-26% B from 15 to 195 min, 90% B from195 to 210 min, 90% B from to 220 min at 300nl/min, and back to 1% B from 220 to 275 at 500 nl/min. The analytical column was connected to a Nanospray Ion Source (Thermo Fisher Scientific, West Palm Beach, FL) on the front end of an Exploris 240 mass spectrometer (Thermo Fisher Scientific, West Palm Beach, Florida). The capillary temperature is set at 275°C and spray voltage optimized. Data-dependent method

settings were: FTMS was 30,000 resolution from 300 to 2000 m/z followed by MSMS scans at 15,000 resolution, FTMS Top10. Activation was CID using a normalized collision energy of 35. The minimal signal required was 5000 and repeated mass exclusion duration of 60 s. For the mammary membrane proteome an older LTQ OrbiTrap Velos Pro (Thermo Fisher Scientific, West Palm Beach, FL) mass spectrophotometer was used using the settings described[30].

Data analysis

Raw data files from the mass spectrometer were inserted into MaxQuant (Version 1.6.7.0) [32]. Variable modifications were oxidation (M), acetyl (Protein N-term), deamidation (NQ), and Phospho (STY). The fixed modification was carbamidomethyl (C). LFQ was used for label-free quantification. Second, peptides and dependent peptides were both searched for using default parameters. The *mouse* reference database was downloaded from Uniprot (July 2020). Data from MaxQuant was loaded into Perseus [33]. Data were filtered by removing proteins that matched the reverse database and those only identified with modified peptides. For quantification, additional filtering of the data was performed. Proteins were excluded if at least one animal did not have a positive quantification number in the duplicates for one day. The median of the technical replicates was then determined.

The data was then transformed into log2. The last data filtering step was that a protein must have a positive quantification number in six animals for at least one day. Missing values were then imputed. A Hawaii plot was generated and differences in protein abundance at several days compared to day 0 were determined. These protein abundance differences were expressed as a log2 number, and we included only those proteins with a FDR of $P \leq 0.01$ as significant. Because of the above criteria, we did not institute a fold change cutoff. However, all significant protein changes in Supplementary Tables 1 and 2 are at least 1.5-fold change or higher. Our protein abundance measures were greater than a 2-fold change or greater for 95% of proteins whose abundance was significantly changed.

The mass spectrometry proteomics data have been deposited to the ProteomeXchange Consortium[34] via the PRIDE[35] partner repository with the dataset identifier PXD027860. Reviewer account details:

Username

reviewer_pxd027860@ebi.ac.uk

Password

JJqLW4yc

Statistics

We used GraphPad Prism Version 8 (GraphPad Software, San Diego, CA) for the statistical analyses with $P \leq 0.05$ required for significance for the various measurements made. An ordinary one-way ANOVA was used, and Dunnett's multiple comparison test was used to compare HET and KO result to WT. Perseus was used to perform statistical analysis for proteome data.

Declarations

Declaration of competing interest:

None

Author contributions statement:

Timothy A Reinhardt, Conceptualization; Timothy A Reinhardt and John D Lippolis, Data collection; Timothy A Reinhardt, analysis; Timothy A Reinhardt and John D Lippolis, Funding acquisition; Timothy A Reinhardt, Methodology; Mitch Palmer, Histopathology and Histomorphometrically; John Lippolis, Proteomics; Timothy A Reinhardt, Project administration; Timothy A Reinhardt and John D Lippolis, Resources; Timothy A Reinhardt, Supervision; Timothy A Reinhardt, Roles/Writing original draft; Timothy A Reinhardt; John D Lippolis and Mitch Palmer, editing.

Funding:

This research was funded solely by the United States Department of Agriculture Research Service (USDA/ARS), Project number 3625-32000-115-000

Acknowledgments:

We thank Tera Nyholm and Duane Zimmerman for animal sampling and technical expertise. ICPMS measurements were performed in the Oregon Health & Science University Elemental Analysis Core facility with partial support from NIH (S10RR025512). Wish me (TAR) happy retirement after this is published.

References

1. Horst, R. L., Goff, J. P. & Reinhardt, T. A. Adapting to the transition between gestation and lactation: differences between rat, human and dairy cow. *Journal of mammary gland biology and neoplasia*, **10**, 141–156 (2005).
2. Baumrucker, C. R. in Lactation: A Comprehensive Treatise Vol. Volume 4 (ed B.L. Larson)463–474. (Academic Press, Inc., 1978).
3. Neville, M. C. & Peaker, M. Calcium fluxes in mouse mammary tissue in vitro: intracellular and extracellular calcium pools. *Journal of Physiology*, **323**, 497–517 (1982).
4. Reinhardt, T. A., Lippolis, J. D., Shull, G. E. & Horst, R. L. Null mutation in the gene encoding plasma membrane Ca2+-ATPase isoform 2 impairs calcium transport into milk. *J Biol Chem*, **279**, 42369–42373 (2004).
5. VanHouten, J. N., Neville, M. C. & Wysolmerski, J. J. The calcium-sensing receptor regulates plasma membrane calcium adenosine triphosphatase isoform 2 activity in mammary epithelial cells: a mechanism for calcium-regulated calcium transport into milk., **148**, 5943–5954 (2007).
6. Cross, B. M., Hack, A., Reinhardt, T. A. & Rao, R. SPCA2 regulates Orai1 trafficking and store independent Ca2 + entry in a model of lactation. *PloS one*, **8**, e67348 https://doi.org/10.1371/journal.pone.0067348 (2013).
7. Reinhardt, T. A., Lippolis, J. D. & Sacco, R. E. The Ca(2+)/H(+) antiporter TMEM165 expression, localization in the developing, lactating and involuting mammary gland parallels the secretory

pathway Ca(2+) ATPase (SPCA1). *Biochem. Biophys. Res. Commun*, **445**, 417–421 https://doi.org/10.1016/j.bbrc.2014.02.020 (2014).

8. Snyder, N. A., Palmer, M. V., Reinhardt, T. A. & Cunningham, K. W. Milk biosynthesis requires the Golgi cation exchanger TMEM165. *J Biol Chem*, **294**, 3181–3191 https://doi.org/10.1074/jbc.RA118.006270 (2019).
9. Davis, F. M. *et al.* Essential role of Orai1 store-operated calcium channels in lactation. *Proceedings of the National Academy of Sciences of the United States of America*, **112**, 5827–5832 https://doi.org/10.1073/pnas.1502264112 (2015).
10. Feng, M. *et al.* Store-independent activation of Orai1 by SPCA2 in mammary tumors., **143**, 84–98 https://doi.org/10.1016/j.cell.2010.08.040 (2010).
11. Clapham, D. E. Calcium signaling., **131**, 1047–1058 (2007).
12. Cross, B. M., Breitwieser, G. E., Reinhardt, T. A. & Rao, R. Cellular Calcium Dynamics in Lactation and Breast Cancer: From Physiology to Pathology. *Am J Physiol Cell Physiol*, https://doi.org/10.1152/ajpcell.00330.2013 (2013).
13. Grinman, D., Athonvarungkul, D., Wysolmerski, J. & Jeong, J. Calcium Metabolism and Breast Cancer: Echoes of Lactation? *Curr Opin Endocr Metab Res*, **15**, 63–70 https://doi.org/10.1016/j.coemr.2020.11.006 (2020).
14. Xiang, M., Mohamalawari, D. & Rao, R. A novel isoform of the secretory pathway Ca2+,Mn(2+)-ATPase, hSPCA2, has unusual properties and is expressed in the brain. *J Biol Chem*, **280**, 11608–11614 https://doi.org/10.1074/jbc.M413116200 (2005).
15. Vanoevelen, J. *et al.* The secretory pathway Ca2+/Mn2+-ATPase 2 is a Golgi-localized pump with high affinity for Ca2 + ions. *J Biol Chem*, **280**, 22800–22808 https://doi.org/10.1074/jbc.M501026200 (2005).
16. Reinhardt, T. A. & Lippolis, J. D. Mammary gland involution is associated with rapid down regulation of major mammary Ca2+-ATPases. *Biochemical and biophysical research communications*, **378**, 99–102 https://doi.org/10.1016/j.bbrc.2008.11.004 (2009).
17. Reinhardt, T. A., Filoteo, A. G., Penniston, J. T. & Horst, R. L. Ca(2+)-ATPase protein expression in mammary tissue. *Am J Physiol Cell Physiol*, **279**, C1595–1602 (2000).
18. Okunade, G. W. *et al.* Loss of the Atp2c1 secretory pathway Ca(2+)-ATPase (SPCA1) in mice causes Golgi stress, apoptosis, and midgestational death in homozygous embryos and squamous cell tumors in adult heterozygotes. *J Biol Chem*, **282**, 26517–26527 https://doi.org/10.1074/jbc.M703029200 (2007).
19. McAndrew, D. *et al.* ORAI1-mediated calcium influx in lactation and in breast cancer. *Mol Cancer Ther*, **10**, 448–460 https://doi.org/10.1158/1535-7163.MCT-10-0923 (2011).
20. van Roy, F. & Berx, G. The cell-cell adhesion molecule E-cadherin. *Cell Mol Life Sci*, **65**, 3756–3788 https://doi.org/10.1007/s00018-008-8281-1 (2008).
21. Dang, D. K. *et al.* A Ca(2+)-ATPase Regulates E-cadherin Biogenesis and Epithelial-Mesenchymal Transition in Breast Cancer Cells. *Mol Cancer Res*, **17**, 1735–1747 https://doi.org/10.1158/1541-

7786.MCR-19-0070 (2019).

22. Reinhardt, T. A., Horst, R. L. & Waters, W. R. Characterization of Cos-7 cells overexpressing the rat secretory pathway Ca2+-ATPase. *Am J Physiol Cell Physiol*, **286**, C164–169 (2004).
23. Nemir, M. *et al.* Targeted inhibition of osteopontin expression in the mammary gland causes abnormal morphogenesis and lactation deficiency. *J Biol Chem*, **275**, 969–976 https://doi.org/10.1074/jbc.275.2.969 (2000).
24. Zeyda, M. *et al.* Osteopontin is an activator of human adipose tissue macrophages and directly affects adipocyte function., **152**, 2219–2227 https://doi.org/10.1210/en.2010-1328 (2011).
25. Tuck, A. B. *et al.* Osteopontin induces increased invasiveness and plasminogen activator expression of human mammary epithelial cells., **18**, 4237–4246 https://doi.org/10.1038/sj.onc.1202799 (1999).
26. El-Tanani, M. K. *et al.* The regulation and role of osteopontin in malignant transformation and cancer. *Cytokine Growth Factor Rev*, **17**, 463–474 https://doi.org/10.1016/j.cytogfr.2006.09.010 (2006).
27. National Research Council (U.S.). *Institute for Laboratory Animal Research (U.S.) & National Academies Press (U.S.). xxv, 220 p* (National Academies Press,, Washington, D.C., 2011). Committee for the Update of the Guide for the Care and Use of Laboratory Animals
28. Percie du Sert. N. et al. The ARRIVE guidelines 2.0: Updated guidelines for reporting animal research. *PLoS Biol*, **18**, e3000410 https://doi.org/10.1371/journal.pbio.3000410 (2020).
29. Lucas, A., Gibbs, J. A., Lyster, R. L. & Baum, J. D. Creamatocrit: simple clinical technique for estimating fat concentration and energy value of human milk. *Br. Med. J*, **1**, 1018–1020 https://doi.org/10.1136/bmj.1.6119.1018 (1978).
30. Reinhardt, T. A. & Lippolis, J. D. Characterization of bovine mammary gland dry secretions and their proteome from the end of lactation through day 21 of the dry period. *J. Proteomics*, **223**, 103831 https://doi.org/10.1016/j.jprot.2020.103831 (2020).
31. Sheehan, D. C. & Hrapchak, B. B. Theory and practice of histotechnology. 2d edn(Mosby, 1980).
32. Cox, J. & Mann, M. MaxQuant enables high peptide identification rates, individualized ppb-range mass accuracies and proteome-wide protein quantification. *Nature biotechnology*, **26**, 1367–1372 (2008).
33. Tyanova, S. *et al.* The Perseus computational platform for comprehensive analysis of (prote) omics data. *Nature methods*, **13**, 731 (2016).
34. Deutsch, E. W. *et al.* The ProteomeXchange consortium in 2020: enabling 'big data' approaches in proteomics. *Nucleic Acids Res*, **48**, D1145–D1152 https://doi.org/10.1093/nar/gkz984 (2020).
35. Perez-Riverol, Y. *et al.* The PRIDE database and related tools and resources in 2019: improving support for quantification data. *Nucleic Acids Res*, **47**, D442–D450 https://doi.org/10.1093/nar/gky1106 (2019).

Figures

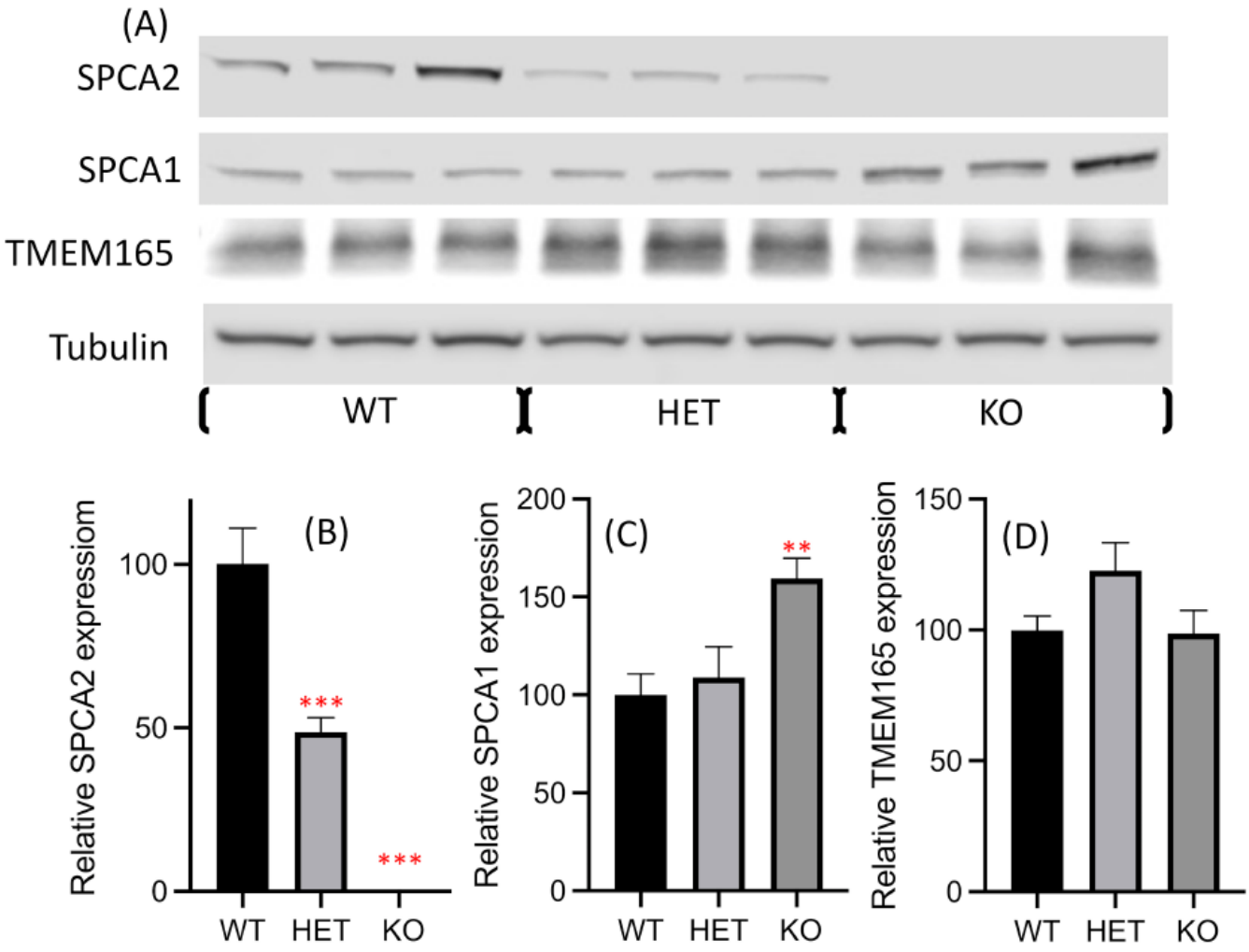

Figure 1

Panel A shows SPCA2, SPCA1 and TMEM165 in representative western blots for all 3 SPCA2 genotypes using tissue from day 13 of lactation. Panel B shows SPCA2 relative expression corrected for tubulin for all 3 SPCA2 genotypes using tissue from day 13 of lactation. Panel C shows SPCA1 relative expression corrected for tubulin for all 3 SPCA2 genotypes using tissue from day 13 of lactation. Panel D shows TMEM165 relative expression corrected for tubulin for all 3 SPCA2 genotypes using tissue from day 13 of lactation. The blot pictures shown in this figure were cropped from a full-size gel for presentation purposes. The full-size gels from which crop images were prepared to make this figure can be seen in Supplementary Figure 1 full-size gels. Mean ± SEM, n = 6 lactating mothers. *** $P \leq 0.001$, ** $P \leq 0.01$ and * $P \leq 0.05$.

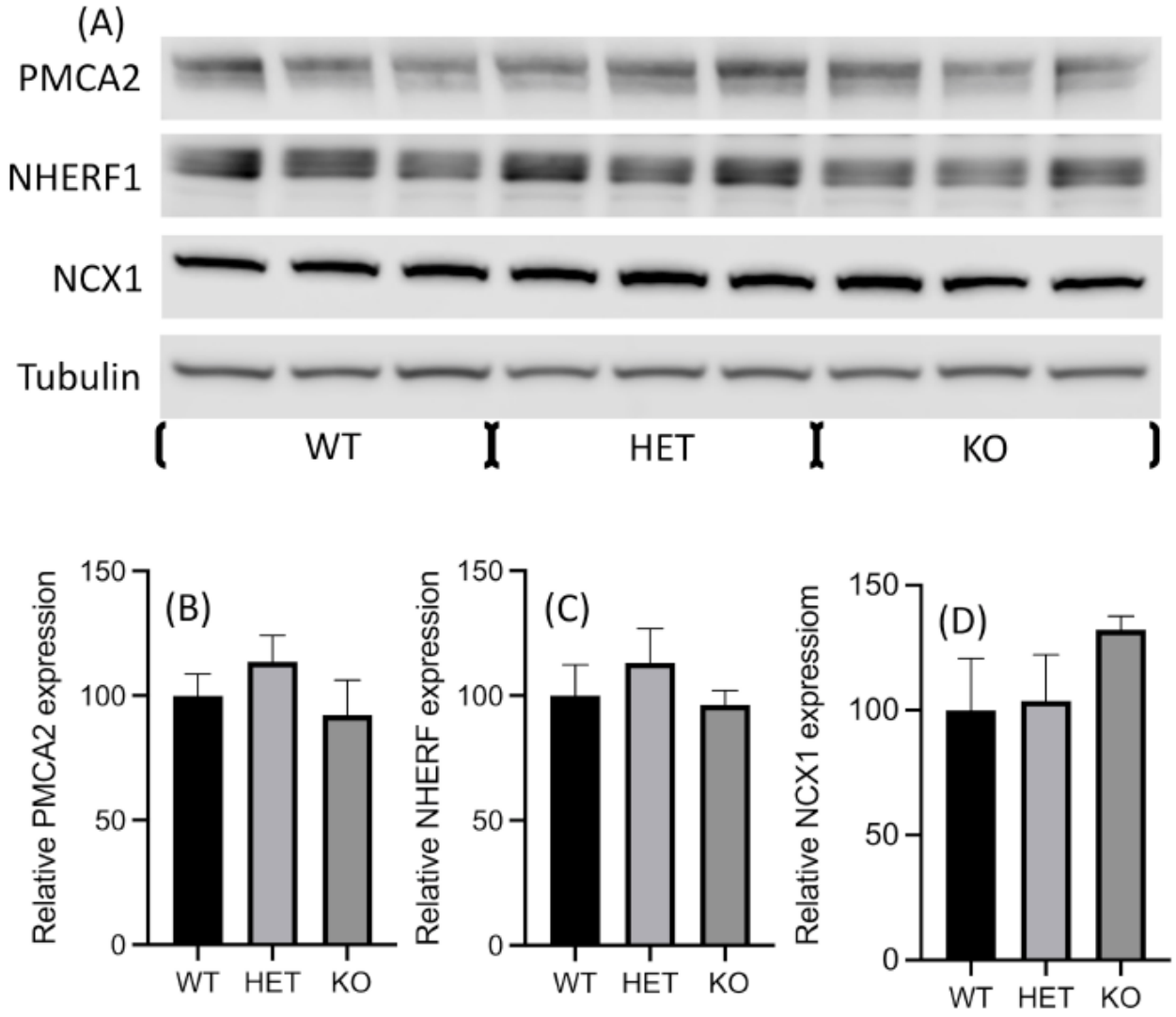

Figure 2

Panel A shows PMCA2, NHREF1 and NCX1 in representative western blots for all 3 SPCA2 genotypes using tissue from day 13 of lactation. Panel B shows PMCA2 relative expression corrected for tubulin for all 3 SPCA2 genotypes using tissue from day 13 of lactation. Panel C shows NHREF1 relative expression corrected for tubulin for all 3 SPCA2 genotypes using tissue from day 13 of lactation. Panel D shows NCX1 relative expression corrected for tubulin for all 3 SPCA2 genotypes using tissue from day 13 of lactation. The blot pictures shown in this figure were cropped from a full-size gel for presentation purposes. The full-size gels from which crop images were prepared to make this figure can be seen in Supplementary Figure 1 full-size gels. Mean ± SEM, n = 6 lactating mothers. *** $P \leq 0.001$, ** $P \leq 0.01$ and * $P \leq 0.05$.

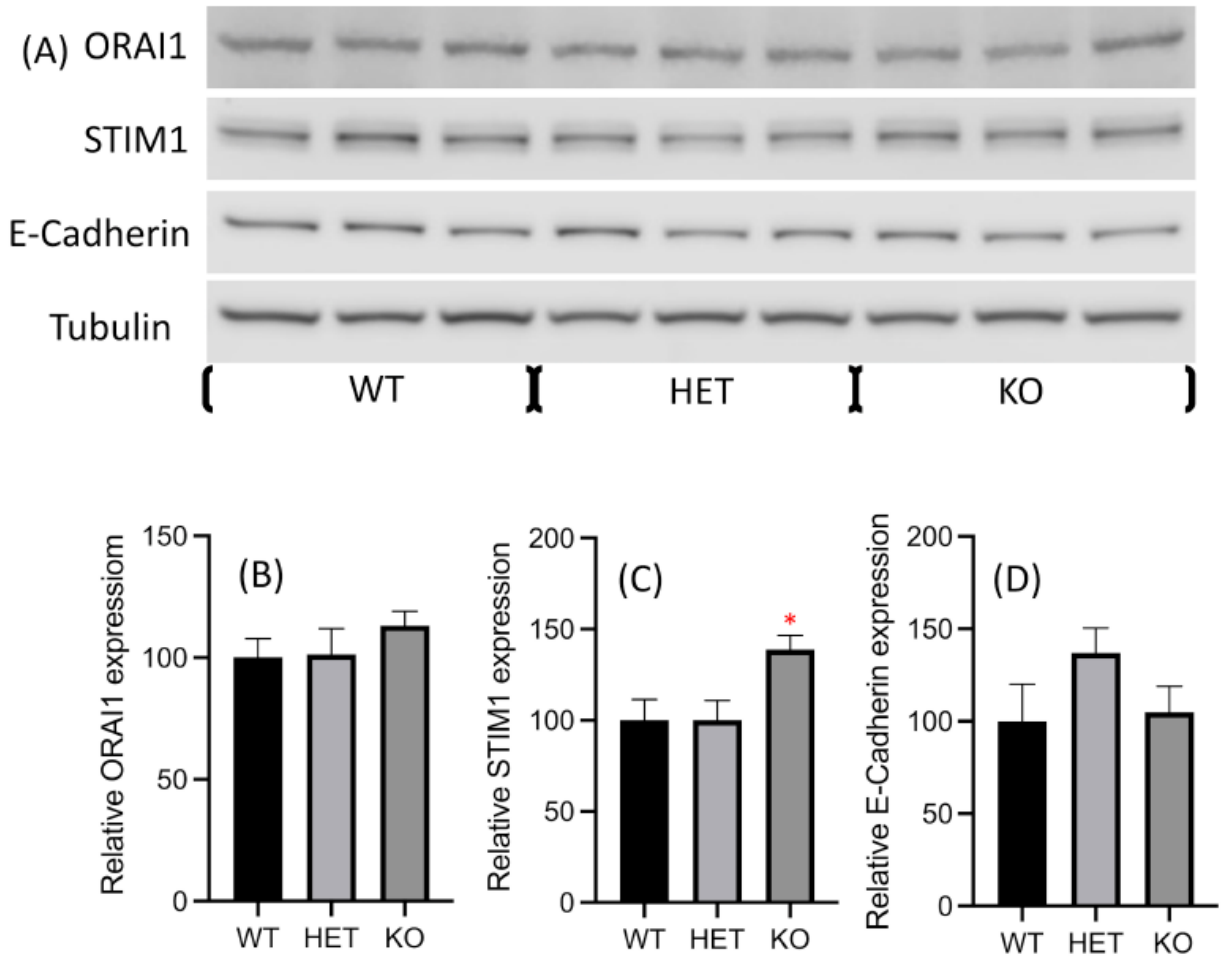

Figure 3

Panel A shows ORAI1, STIM1, Osteopontin, and E-Cadherin in representative western blots for all 3 SPCA2 genotypes using tissue from day 13 of lactation. Panel B shows ORAI1 relative expression corrected for tubulin for all 3 SPCA2 genotypes using tissue from day 13 of lactation. Panel C shows STIM1 relative expression corrected for tubulin for all 3 SPCA2 genotypes using tissue from day 13 of lactation. Panel D shows Osteopontin relative expression corrected for tubulin for all 3 SPCA2 genotypes using tissue from day 13 of lactation. Panel E shows E-Cadherin relative expression corrected for tubulin for all 3 SPCA2 genotypes using tissue from day 13 of lactation. The blot pictures shown in this figure were cropped from a full-size gel for presentation purposes. The full-size gels from which crop images were prepared to make this figure can be seen in Supplementary Figure 1 full-size gels. Mean ± SEM, n = 6 lactating mothers. *** $P \leq 0.001$, ** $P \leq 0.01$ and * $P \leq 0.05$.

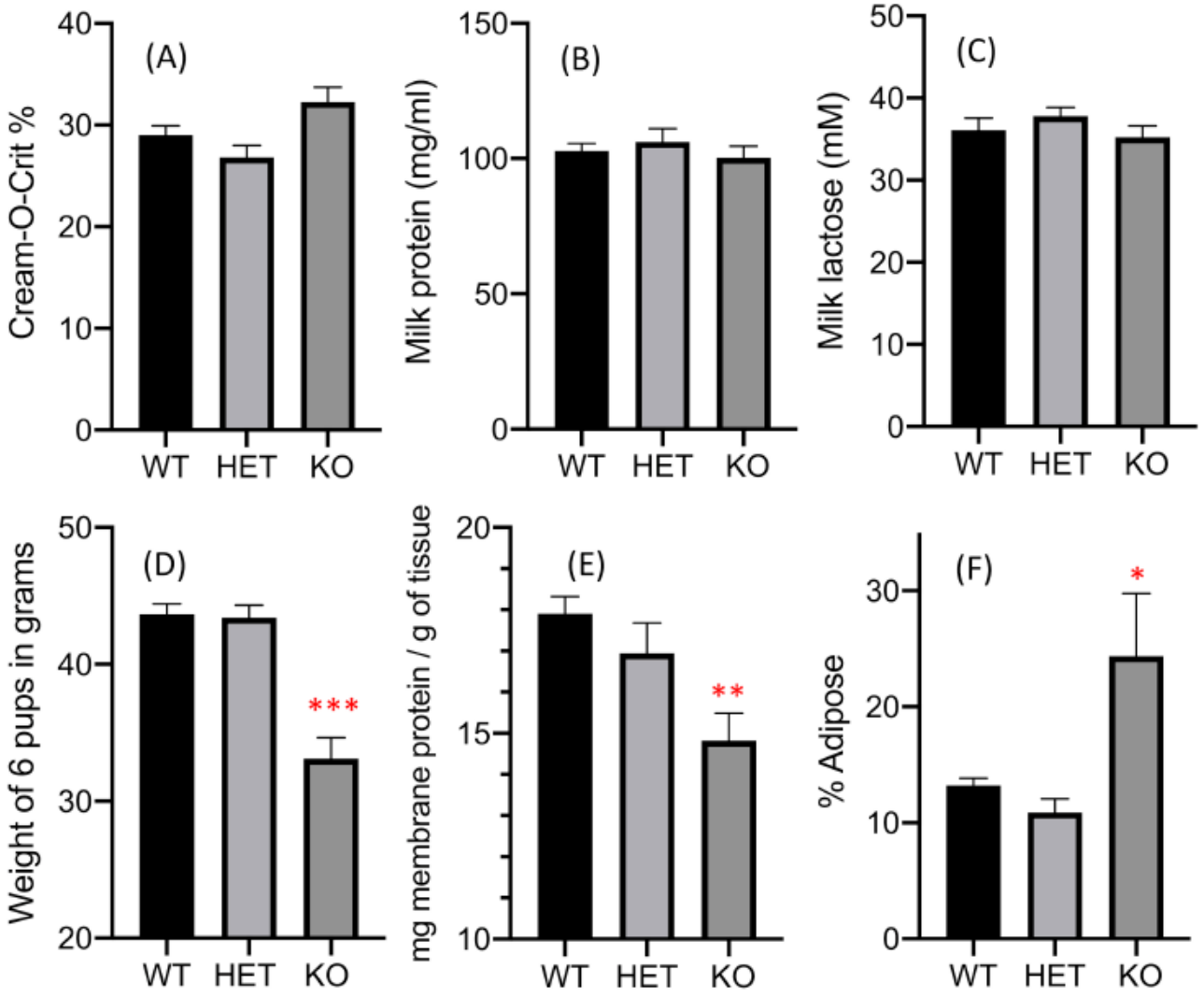

Figure 4

Panels A, B, and C show cream-o-crit, milk protein and milk lactose, respectively, by genotype. None of these milk component measures was affected by the loss of SPCA2. An indirect measure of milk production is pup weight. The weight of six pup groups from each SPCA2 genotype on day 12 of lactation is shown in Figure 3D. Figure 3E shows mg of crude membrane protein isolated from one gram of lactating mammary tissue from each SPCA2 genotype at day 12 of lactation. Figure 3F shows % adipose tissue present in histological sections from each SPCA2 genotype on day 13 of lactation. Mean ± SEM, n = 6 lactating mothers. *** $P \leq 0.001$, ** $P \leq 0.01$ and * $P \leq 0.05$.

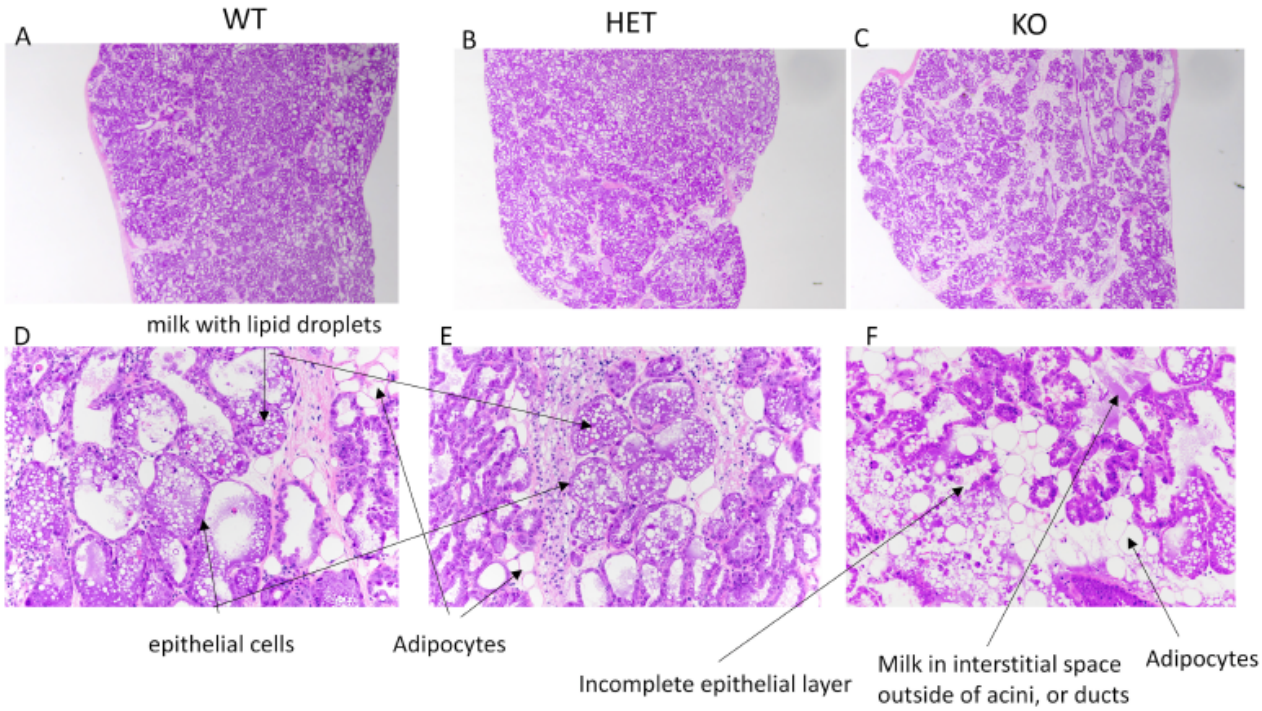

Figure 5

Sections of mouse mammary gland from wild-type (A), SPCA2 heterozygous (B), and SPCA2 KO (C) mice. Note increased interstitial stroma and adipose tissue present in the mammary gland from SPCA2 KO compared to wild-type or SPCA2 heterozygous mice. Alveoli of wild-type (C), SPCA2 heterozygous (B), and SPCA2 KO (C) mice have alveoli lined by cuboidal, pyramidal, or flattened epithelial cells, some of which contain large vacuoles. Alveolar lumens contain variable amounts of milk with lipid droplets. In the mammary gland from SPCA2 KO mice, there are increases in the stroma and adipose tissue. Milk is within the interstitial space and outside of alveoli or ducts, resulting in direct connections between alveoli with incomplete epithelial lining and the interstitial space (E).

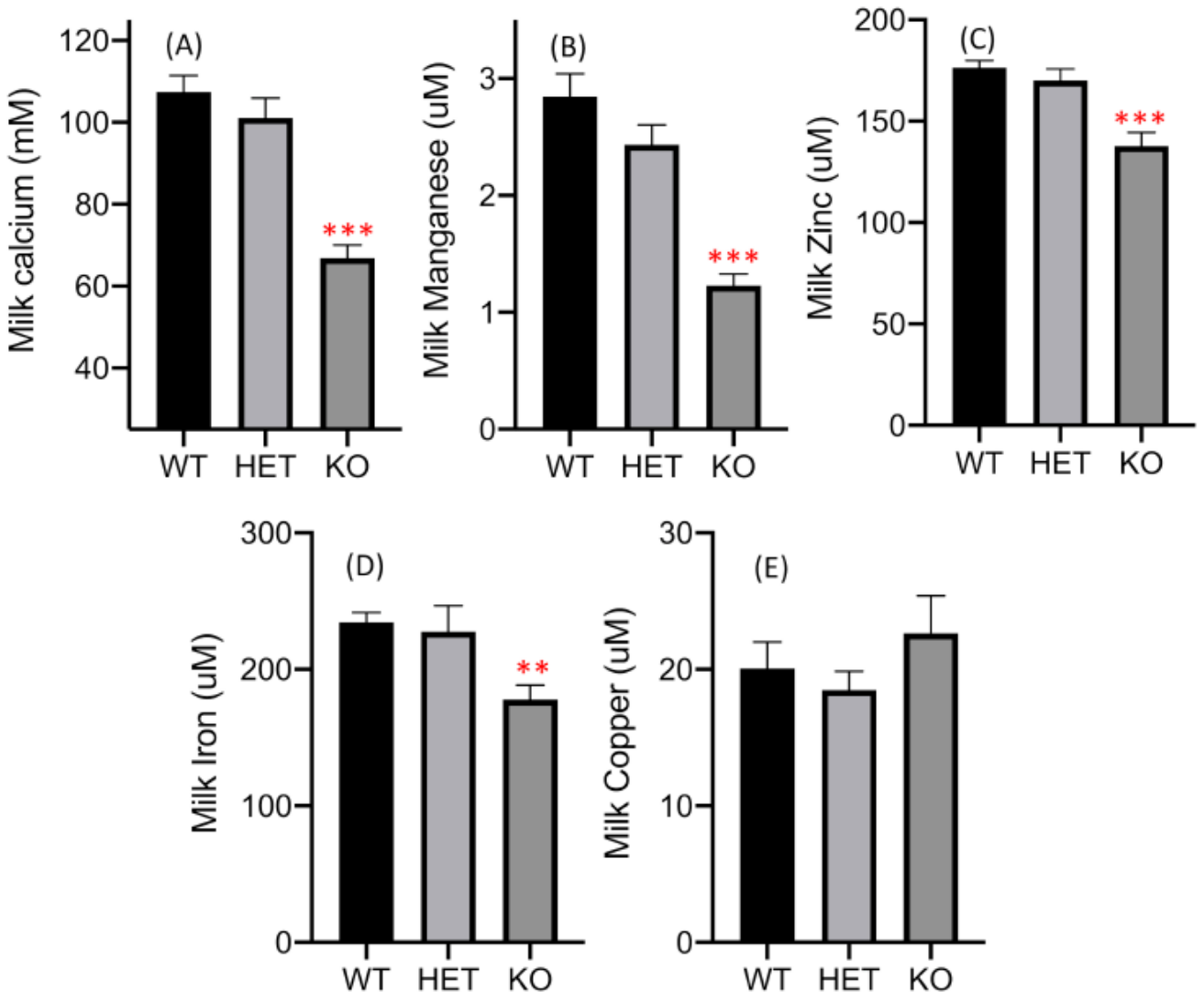

Figure 6

Milk mineral concentrations are presented for all three SPCA2 genotypes. Panel A. Day 12 milk calcium concentrations. Panel B. Day 12 milk manganese concentrations. Panel C. Day 12 milk zinc concentrations. Panel D. Day 12 milk iron concentrations. Panel E. Day 12 milk copper concentrations. Mean ± SEM, n = 6 lactating mothers. *** $P \leq 0.001$, ** $P \leq 0.01$ and * $P \leq 0.05$.

Supplementary Files

This is a list of supplementary files associated with this preprint. Click to download.

- Supplementarydatatable1MouseMammaryproteome.xlsx

- Supplementarydatatable2MouseMilkproteome.xlsx
- Supplementarydatatable3MouseMammaryMembraneproteome.xlsx
- SupplimentarydatafilesLegends.docx
- SupplimentalFigure1fullsizegels.pdf